JOURNAL OF
Applied Polymer
SCIENCE

Special Issue: Polymers for Microelectronics

Guest Editors: Dr Brian Knapp (Promerus LLC) and
Prof. Paul A. Kohl (Georgia Institute of Technology)

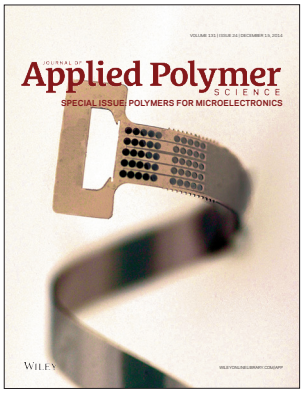

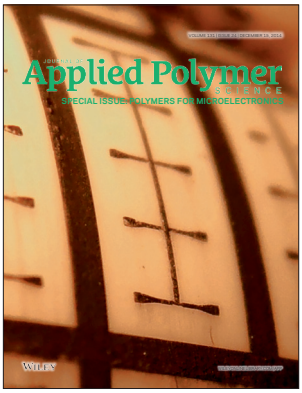

EDITORIAL

Polymers for Microelectronics
B. Knapp and P. A. Kohl, *J. Appl. Polym. Sci.* 2014, **DOI: 10.1002/app.41233**

REVIEW

Negative differential conductance materials for flexible electronics
A. Nogaret, *J. Appl. Polym. Sci.* 2014, **DOI: 10.1002/app.40169**

RESEARCH ARTICLES

Generic roll-to-roll compatible method for insolubilizing and stabilizing conjugated active layers based on low energy electron irradiation
M. Helgesen, J. E. Carlé, J. Helt-Hansen, A. Miller, and F. C. Krebs, *J. Appl. Polym. Sci.* 2014, **DOI: 10.1002/app.40795**

Selective etching of polylactic acid in poly(styrene)-block-poly(D,L)lactide diblock copolymer for nanoscale patterning
C. Cummins, P. Mokarian-Tabari, J. D. Holmes, and M. A. Morris, *J. Appl. Polym. Sci.* 2014, **DOI: 10.1002/app.40798**

Preparation and dielectric behavior of polyvinylidene fluoride composite filled with modified graphite nanoplatelet
P. Xie, Y. Li, and J. Qiu, *J. Appl. Polym. Sci.* 2014, **DOI: 10.1002/app.40229**

Design of a nanostructured electromagnetic polyaniline–Keggin iron–clay composite modified electrochemical sensor for the nanomolar detection of ascorbic acid
R. V. Lilly, S. J. Devaki, R. K. Narayanan, and N. K. Sadanandhan, *J. Appl. Polym. Sci.* 2014, **DOI: 10.1002/app.40936**

Synthesis and characterization of novel phosphorous-silicone-nitrogen flame retardant and evaluation of its flame retardancy for epoxy thermosets
Z.-S. Li, J.-G. Liu, T. Song, D.-X. Shen, and S.-Y. Yang, *J. Appl. Polym. Sci.* 2014, **DOI: 10.1002/app.40412**

Electrical percolation behavior and electromagnetic shielding effectiveness of polyimide nanocomposites filled with carbon nanofibers
L. Nayak, T. K. Chaki, and D. Khastgir, *J. Appl. Polym. Sci.* 2014, **DOI: 10.1002/app.40914**

Morphological influence of carbon modifiers on the electromagnetic shielding of their linear low density polyethylene composites
B. S. Villacorta and A. A. Ogale, *J. Appl. Polym. Sci.* 2014, **DOI: 10.1002/app.41055**

Electrical and EMI shielding characterization of multiwalled carbon nanotube/polystyrene composites
V. K. Sachdev, S. Bhattacharya, K. Patel, S. K. Sharma, N. C. Mehra, and R. P. Tandon, *J. Appl. Polym. Sci.* 2014, **DOI: 10.1002/app.40201**

Anomalous water absorption by microelectronic encapsulants due to hygrothermal-induced degradation
M. van Soestbergen and A. Mavinkurve, *J. Appl. Polym. Sci.* 2014, **DOI: 10.1002/app.41192**

Design of cyanate ester/azomethine/ZrO_2 nanocomposites high-k dielectric materials by single step sol-gel approach
M. Ariraman, R. Sasi Kumar and M. Alagar, *J. Appl. Polym. Sci.* 2014, **DOI: 10.1002/app.41097**

Furan/imide Diels–Alder polymers as dielectric materials
R. G. Lorenzini and G. A. Sotzing, *J. Appl. Polym. Sci.* 2014, **DOI: 10.1002/app.40179**

High dielectric constant polyimide derived from 5,5'-bis[(4-amino) phenoxy]-2,2'-bipyrimidine
X. Peng, Q. Wu, S. Jiang, M. Hanif, S. Chen, and H. Hou, *J. Appl. Polym. Sci.* 2014, **DOI: 10.1002/app.40828**

The influence of rigid and flexible monomers on the physical-chemical properties of polyimides
T. F. da Conceição and M. I. Felisberti, *J. Appl. Polym. Sci.* 2014, **DOI: 10.1002/app.40351**

JOURNAL OF
Applied Polymer
SCIENCE

Special Issue: Polymers for Microelectronics

Guest Editors: Dr Brian Knapp (Promerus LLC) and
Prof. Paul A. Kohl (Georgia Institute of Technology)

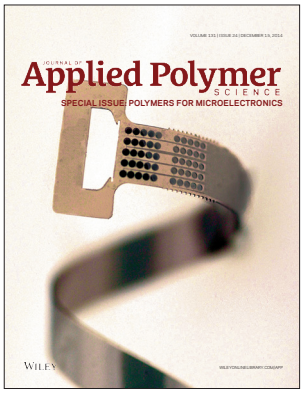

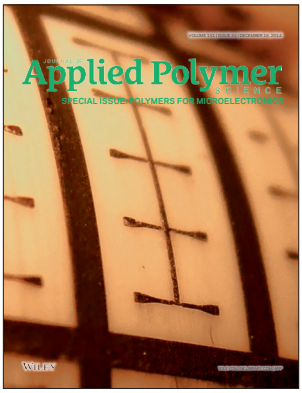

Development of polynorbornene as a structural material for microfluidics and flexible BioMEMS
A. E. Hess-Dunning, R. L. Smith, and C. A. Zorman, *J. Appl. Polym. Sci.* 2014, **DOI:** 10.1002/app.40969

A thin film encapsulation layer fabricated via initiated chemical vapor deposition and atomic layer deposition
B. J. Kim, D. H. Kim, S. Y. Kang, S. D. Ahn, and S. G. Im, *J. Appl. Polym. Sci.* 2014, **DOI:** 10.1002/app.40974

Surface relief gratings induced by pulsed laser irradiation in low glass-transition temperature azopolysiloxanes
V. Damian, E. Resmerita, I. Stoica, C. Ibanescu, L. Sacarescu, L. Rocha, and N. Hurduc, *J. Appl. Polym. Sci.* 2014, **DOI:** 10.1002/app.41015

Polymer-based route to ferroelectric lead strontium titanate thin films
M. Benkler, J. Hobmaier, U. Gleißner, A. Medesi, D. Hertkorn, and T. Hanemann, *J. Appl. Polym. Sci.* 2014, **DOI:** 10.1002/app.40901

The influence of dispersants that contain polyethylene oxide groups on the electrical resistivity of silver paste
T. H. Chiang, Y.-F. Chen, Y. C. Lin, and E. Y. Chen, *J. Appl. Polym. Sci.* 2014, **DOI:** 10.1002/app.41183

Quantitative investigation of the adhesion strength between an SU-8 photoresist and a metal substrate by scratch tests
X. Zhang, L. Du, and M. Zhao, *J. Appl. Polym. Sci.* 2014, **DOI:** 10.1002/app.41108

Thermodynamic and kinetic aspects of defectivity in directed self-assembly of cylinder-forming diblock copolymers in laterally confining thin channels
B. Kim, N. Laachi, K. T. Delaney, M. Carilli, E. J. Kramer, and G. H. Fredrickson, *J. Appl. Polym. Sci.* 2014, **DOI:** 10.1002/app.40790

JOURNAL OF Applied Polymer SCIENCE

A Thin Film Encapsulation Layer Fabricated via Initiated Chemical Vapor Deposition and Atomic Layer Deposition

Bong Jun Kim,[1] Do Heung Kim,[1] Seung Youl Kang,[2] Seong Deok Ahn,[2] Sung Gap Im[1]

[1]Department of Chemical and Biomolecular Engineering & Graphene Research Center, KI for Nanocentury, KAIST, Daejeon 305-701, Republic of Korea

[2]Next Generation Display Research Department, Electronics and Telecommunications Research Institute, Yuseong-gu Daejeon 305-700, Republic of Korea

Correspondence to: S. G. Im (E-mail: sgim@kaist.ac.kr)

ABSTRACT: An organic/inorganic hybrid multilayer for encapsulation of organic electronic devices is developed, where the organic polymer layer and the inorganic layer are alternatively deposited by initiated chemical vapor deposition and atomic layer deposition processes, respectively. The thickness of each organic and inorganic layer is optimized to minimize the water vapor transmission rate (WVTR) determined by a Ca test. The produced barrier film shows an outstanding optical property as its light transmittance is average 89.42% at visible light region. The WVTR of the developed thin film encapsulation layer is as low as 2.17×10^{-4} g m^{-2} day^{-1} at 38°C, 90% relative humidity (RH). This value is equivalent to 1.29×10^{-5} g m^{-2} day^{-1} at ambient condition, which is sufficient to elongate the lifetime of organic electronic devices. © 2014 Wiley Periodicals, Inc. J. Appl. Polym. Sci. **2014**, *131*, 40974.

KEYWORDS: films; property relations; radical polymerization; structure

Received 26 February 2014; accepted 14 May 2014
DOI: 10.1002/app.40974

INTRODUCTION

Organic electronic devices have attracted huge interest from both academia and industry, due to the advantageous features such as low manufacturing cost and superb mechanical flexibility, as well as their high electronic performance. They are recognized as one of the strongest candidate devices for future electronics with various interesting aspects which are extremely hard to achieve with the current devices: extremely thin, flexible, light/portable, and wearable/embeddable. However, one of the most critical shortcomings of organic electronic devices is their vulnerability to the operational environment. Especially, upon their exposure to water vapor and/or oxygen, the organic electronic devices tend to degrade rapidly, and the devices become non-operational just within few hours or days.[1] Therefore, an encapsulation must be applied to the organic electronic devices to block the penetration of water vapor and oxygen to the device for the development of the reliable organic electronics products. The water vapor transmission rate (WVTR) value of 10^{-6} g m^{-2} day^{-1} is generally required to guarantee a sufficient encapsulation of organic light emitting diode (OLED),[2] while relatively moderate demand (WVTR value of 10^{-3} g m^{-2} day^{-1} or less) is expected for organic photovoltaics (OPV) or organic thin film transistors (OTFT).[3] To satisfy such demanding WVTR requirements, various types of encapsulation barrier system with outstanding performance were devised; attaching glass or metal lid to the devices had shown to be an effective method, which is quite simple to perform and shows excellent encapsulation performance.[4] However, this approach is not compatible with flexible applications, one of the most differentiated characteristics of the organic electronic devices. Thus, thin film barrier encapsulation have been extensively investigated to satisfy the flexibility requirement.[5–7]

Here, we developed a novel fabrication method of organic/inorganic hybrid multilayer system for the encapsulation of organic electronic devices. For the multilayer stacking, initiated chemical vapor deposition (iCVD) and atomic layer deposition (ALD) were adapted for the deposition of organic polymer layer and inorganic oxide layer, respectively. The iCVD is a process that uses thermally induced radicals for the initiation of surface polymerization, resulting in a thin polymer film with extreme conformality and high polymer purity.[8] In the iCVD process, vaporized initiator and monomer are introduced into the reaction chamber. A thermal cracking of the introduced initiators by the hot filament placed in the chamber forms radicals. The radicals attack the vinyl groups of the vaporized monomers to form monomer radicals and the chain reaction of radical polymerization takes place on the surface of the substrate to produce organic polymer film.[9] iCVD process does not damage the substrate since it is a solvent-less vapor phase deposition, and the substrate temperature is near

room temperature of 10–40°C.[10] With such characteristics, iCVD has been applied to fabricate multilayers for barrier purpose. iCVD polymer layer was used to successfully fill the nano-porosity of inorganic layer deposited via plasma-enhanced chemical vapor deposition (PECVD),[11] and single-chamber process of multilayer fabrication using iCVD and PECVD systems was developed to produce organic/inorganic hybrid multilayer.[12] Recently, iCVD was coupled with plasma-enhanced ALD (PEALD) as well.[13] This research combined the iCVD organic layer with thermal ALD system, and deduced the optimized thickness of the iCVD layer for the first time. Along with the previous researches, this paper can further prove the applicability of iCVD organic layer to barrier application. ALD, which is widely used for the production of encapsulation barrier films, can produce pinhole-free oxide films with outstanding smoothness and conformality that serves as excellent barrier film.[14] Both iCVD and ALD processes are conducted in vapor phase that does not require the use of additional solvents that might cause damage to organic electronic devices. In this research, organic/inorganic hybrid multilayer is fabricated via alternating deposition of iCVD and ALD, and the multilayer structure was optimized to achieve a maximized barrier performance. The optical transparency and surface properties were also investigated and a recently developed calcium (Ca) test method was utilized to evaluate the WVTR of the hybrid multilayer system. The outstanding encapsulation performance achieved in this work will prompt the advance of the organic electronics industry by rendering a substantially improved reliability and elongated lifetime.

EXPERIMENTAL

Organic Layer Deposition via iCVD

The organic layer used in this work was poly(2,4,6,8-tetravinyl-2,4,6,8-tetramethylcyclotetrasiloxane) (pV4D4). It was deposited by a vapor-phase polymerization of 2,4,6,8-tetravinyl-2,4,6,8-tetramethylcyclotetrasiloxane (V4D4) (97%, Tokyo Chemical Industry, Tokyo, Japan) via custom-built iCVD system (Daeki Hi-Tech, Daejeon, Korea). V4D4 monomer was filled in a source cylinder in the iCVD system and was heated to 70°C to vaporize the V4D4 monomer. The initiator used in this work was *tert*-butyl peroxide (TBPO) (98%, Sigma-Aldrich, St. Louis, USA). TBPO is sufficiently volatile at room temperature and desired flow of TBPO vapor could be obtained without additional heating. All the chemicals used in this work were used as received without any further purification. The vaporized initiator and monomer were introduced into the iCVD chamber with the flow rate about 1 standard cubic centimeter per minute (sccm) for each substance. The filament temperature was set to 220°C for the thermal decomposition of TBPO to form free radicals to initiate the polymerization reaction. The process pressure was 250 mTorr, controlled by a proportional-integral-derivative (PID) controller and the substrate temperature was maintained at 40°C using a circulator. The deposition thickness was monitored *in situ* by interferometry.

Inorganic Layer Deposition via ALD

Al_2O_3 was deposited as the inorganic layer in this work by ALD system (LUCIDA D100, NCD, Daejeon, Korea). The chamber temperature was set as 90°C to minimize the thermal effect on organic electronic devices. Within the reactor, two precursors, $Al(CH_3)_3$ (97%, Sigma-Aldrich) and deionized water H_2O, were introduced alternatively with the exposure time of 0.2 s with 10 s of N_2 purging in between the exposure of the precursors. A computer-aided control of the cycle number was applied to obtain precise film thickness.

Organic/Inorganic Hybrid Multilayer Deposition

When fabricating organic/inorganic hybrid multilayer, the depositions of pV4D4 and Al_2O_3 were alternated to produce one to 3 dyads of the multilayer. For the deposition of alternating layer, N_2-filled container was used for the transportation of the substrate between the iCVD and ALD systems.

Analysis of Organic/Inorganic Hybrid Multilayer

The optical transmittances of the films were measured using an UV-vis spectrometer (UV-3600, Shimadzu, Kyoto, Japan). The base was set as air, so the transmittance data includes the decrease in transparency by the 1-mm thick slide glass. The refractive index of the deposited film, n was obtained by use of a spectroscopic ellipsometer (M2000D, J.A. Woollam, Lincoln, USA). The surface images and roughness of the films were measured using an atomic force microscopy (AFM) (XE-100, Park Systems, Suwon, Korea). The cross section image of the organic/inorganic hybrid multilayer was observed by a scanning electron microscope (SEM) (Nova230, FEI, Hillsboro, USA).

Barrier Property Measurement

Ca test was performed to measure the WVTR of the hybrid multilayer. The Ca film is obtained via a custom-built thermal evaporator (Daeki Hi-Tech, Daejeon, Korea) connected to a glove box filled with N_2. The substrate was 1-mm thick slide glass with the dimension of 2.5 × 2.5 cm^2. The base pressure of the deposition chamber was below 2×10^{-6} mTorr. Ca (99.5%, Junsei Chemical, Tokyo, Japan) was resistively heated on a metal boat with the deposition rate of around 1 Å/s. The deposition rate and thickness were monitored *in situ* by quartz crystal microbalance (QCM). The substrate was rotated during the deposition to improve the uniformity of the Ca layer. The final thickness of the Ca layer was 100 nm. On the Ca-deposited substrate, organic/inorganic hybrid multilayer was sequentially deposited with the procedure described above. The procedure was repeated until the desired number of the layer was deposited.

Then the sample was placed under a humidity chamber (TM-EM-065, JEIO Tech, Daejeon, Korea) at 38°C with 90% relative humidity (RH). In each pre-set time, the sample was shortly removed from the chamber, and a digital camera image at each time was taken to monitor the change of the deposited Ca area. The oxidized area of the Ca sample could be obtained using Image J (National Institute of Health, USA) program. The time rate of oxidized area of the Ca sample was calculated afterwards to estimate the WVTR of the encapsulation layer.

RESULTS AND DISCUSSION

Film Properties of Organic and Inorganic Layers

Due to its excellent barrier property, Al_2O_3 layer was selected as an inorganic barrier layer.[15] pV4D4 was chosen as the organic layer because of its extreme smoothness and outstanding optical properties. AFM images of iCVD pV4D4 layer and ALD Al_2O_3 layer are shown in Figure 1(a,b), respectively. The measured root mean square (RMS) roughness values were 0.713 nm for

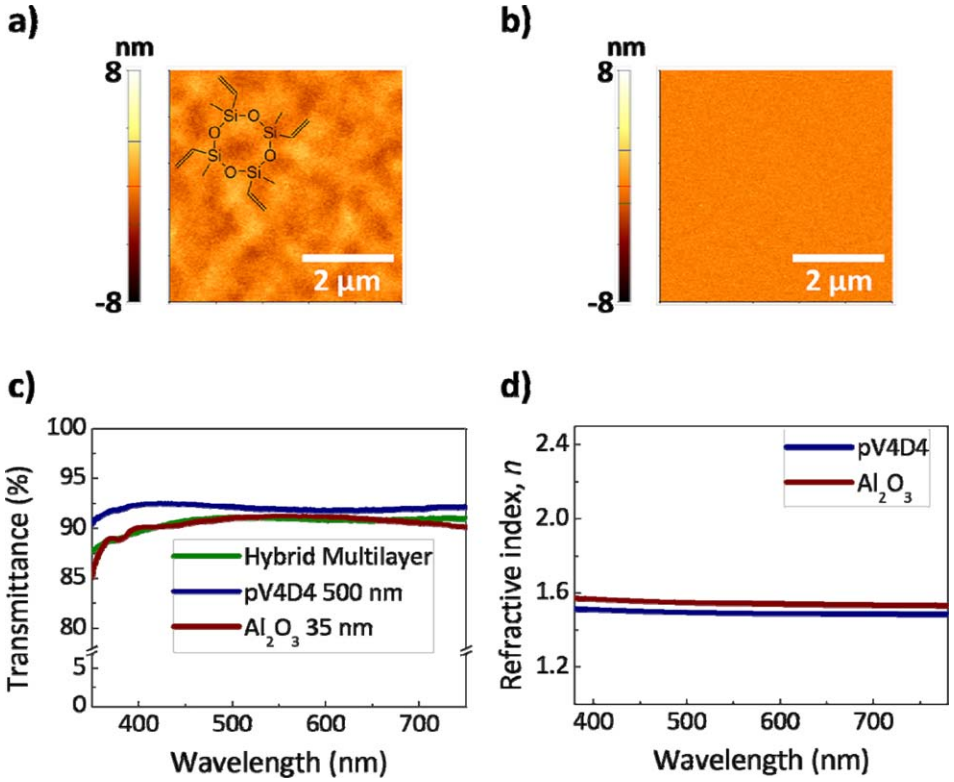

Figure 1. (a) AFM images of iCVD pV4D4 layer (inset image: monomer structure of V4D4) and (b) ALD Al_2O_3 layer on silicon wafer, respectively. (c) Transmittance and (d) refractive index, *n* value of pV4D4 and Al_2O_3 layer, respectively. [Color figure can be viewed in the online issue, which is available at wileyonlinelibrary.com.]

organic layer and 0.141 nm for inorganic layers, indicating that the deposited organic and inorganic films are extremely smooth. Previous reports demonstrated that the roughness of the film is closely related with the barrier property of the encapsulation layers; flatter film exhibited better barrier property because of the easiness in stacking due to flatness.[16] Figure 1(c) shows the light transmittance of the pV4D4, Al_2O_3, and the pV4D4/Al_2O_3 hybrid multilayer. The average transmittance of the 500 nm-thick pV4D4 layer in the visible light region (350–750 nm) was 92.02%. 35-nm thick Al_2O_3 layer had average transmittance of 90.51% in the visible light region. The transmittance value includes the 1 mm thick slide glass used as the substrate, so the transparency of the barrier films alone would be much higher than the measured value illustrated above. Finally, the transmittance of the pV4D4 (500 nm)/Al_2O_3 (35 nm) hybrid multilayer had the average transmittance near 90% with no fluctuation. For the application to the OLEDs and OPVs, high transmittance of multilayer is of significant importance. Figure 1(d) illustrates the refractive index, *n* values of the pV4D4 and Al_2O_3 films. The average *n* value in the visible light region was 1.50 for pV4D4 and 1.55 for Al_2O_3. Since the difference of the refractive index values was as low as 0.05, the additional loss of the light originated from the interference effect could be minimized and no fluctuation of the transmittance data due to cavity effect was observed from the hybrid layer, as shown in Figure 1(c)

Set Up of Ca Test: Oxidized Area Measurement

Ca test was conducted to estimate the WVTR of the encapsulation layer. The WVTR value was calculated according to the method suggested previously by Bertrand et al.[17] Ca was opaque initially, and upon exposure to water vapor and oxygen, it oxidized rapidly and became transparent. Figure 2(a) is the representative digital camera images of the sample under Ca test. After all the digital camera images were collected, the oxidized area percentage of each sample was extracted using Image J program. Figure 2(b) is the representative processed images of the each sample images obtained in Figure 2(a). An exemplary plot is shown in Figure 2(c). The WVTR value could be determined by monitoring the change of the oxidized area percentage of the Ca sample with respect to the time, using the eq. (1).[17]

$$\text{WVTR} \quad [\text{g m}^{-2}\text{day}^{-1}] = n \cdot \delta \cdot \frac{\text{M}(\text{H}_2\text{O})}{\text{M}(\text{Ca})} \cdot h \cdot A \cdot \frac{dA}{dt} \qquad (1)$$

where *n* is the molar equivalent of water molecules to react with one Ca molecule, δ is the density of Ca. M(H_2O) and M(Ca) are the molecular weight of water and Ca, respectively. *h* and *A* are the height and area of the Ca film, respectively. *dA/dt* could be obtained from the linear fit slope of the plotted graph as shown in Figure 2(c). The linear fit was applied to measure the steady state WVTR of the barrier film.[18]

In this work, the encapsulation layer was directly deposited on the Ca layer in an iCVD process chamber attached in N_2-filled glove box. The inert environment during the iCVD process did not oxidize the Ca layer and the organic layer film was successfully integrated without damaging the Ca layer. After the iCVD process, the substrates were delivered using N_2-filled carrier and placed in the ALD system, followed by immediate evacuation of

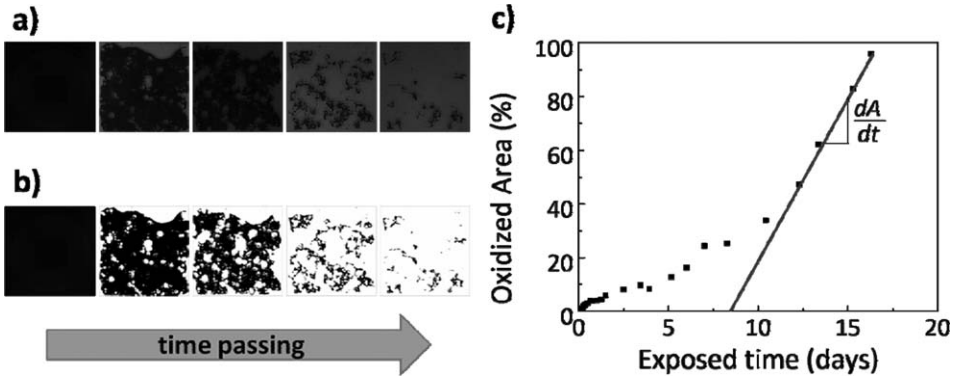

Figure 2. (a) Representative camera images of a sample during the Ca test. (b) Representative processed images of the sample images in a, by Image J. (c) An exemplary graph showing the rate of change of the oxidized area of the sample.

the ALD system. The total exposure time of Ca test film covered with single iCVD layer was no larger than 3–5 s and our result indicates that this short exposure of the sample to the ambient did not cause any significant oxidation of Ca layer. The iCVD polymer layer has poor intrinsic barrier property. However, the barrier property of iCVD layer was sufficient to block the Ca degradation before and during the ALD process. The penetration of the water vapor used during the ALD process could also be blocked by the iCVD polymer layer. Moreover, after only a few ALD cycles, newly added ALD Al_2O_3 layer can block the water penetration and no apparent degradation of Ca layer was observed during the sample preparation procedure.

In most of previously reported conventional optical or electrical Ca test methods, the Ca layer was sealed with an encapsulation layer fabricated on a separate substrate, using epoxy glue. However, sealing with epoxy-glue sealing has a critical drawback; the epoxy glue used to seal the two substrates has WVTR mostly around 10^{-4} g m^{-2} day^{-1}, and below that value, the measurement becomes unreliable,[19] since most of water vapor permeation will occur through the glue-sealed side, not through the barrier film. This problem keeps it extremely difficult to measure the precise WVTR value of a barrier film using glue-sealing method. Thus, in many cases of Ca tests with epoxy-glued samples, the degradation of Ca layer takes place at the edge of the Ca layer first, and the degradation progresses in a shape of concentric circular form, which indicates that the measured degradation rate is not measuring the performance of the encapsulation barrier film, but the diffusion rate of water and/or oxygen through the epoxy glue.[20] Therefore, it is extremely important to develop a new Ca test method to measure an exact WVTR value, especially when the value is extremely low.

The Ca test method suggested in this work has a huge advantage over the conventional methods that the measurement is not affected by the epoxy glue sealing the sides. Figure 2(a) clearly shows that the degradation of Ca film occurred uniformly throughout the area of Ca layer, which strongly infers that the diffusion of water and/oxygen took place through the encapsulation layer, not through the side wall of the Ca layer. This observation demonstrates that the measured WVTR is the real WVTR value of the developed encapsulation layer. The developed Ca test method enables a reliable, direct measurement of the barrier property of the encapsulation layer.

Optimization of the Structure of Organic/Inorganic Hybrid Multilayer

In this work, on the 100-nm thick Ca film, pV4D4 layer was deposited directly using iCVD process, followed by the deposition of Al_2O_3 layer via ALD process. The iCVD system is set up in a N_2-filled glove box with thermal evaporator while ALD system is settled separately. To avoid the exposure of the bare Ca layer in ambient condition, iCVD process was always conducted firstly before the ALD process. The iCVD layer was also expected to block the H_2O molecules used as a precursor during the ALD process of Al_2O_3 deposition.

The thickness of each layer was systematically controlled to optimize the structure of the organic/inorganic hybrid multilayer. The barrier property of the fabricated encapsulation layer was attempted to be maximized while maintaining the minimized total fabrication time.

Figure 3 illustrates the variation of the WVTR with respect to the change of the thickness of each organic and inorganic layer. First, the thickness of the each Al_2O_3 layer was varied and the WVTR value was estimated by the Ca test suggested above. Parallel with previous studies,[21] the WVTR value of the film decreased exponentially with the increase of the Al_2O_3 layer thickness from 15 to 35 nm, as is shown in Figure 3(a). Since the ALD process is a time consuming process—deposition of 35 nm takes 2 h, thicker deposition was not conducted and the Al_2O_3 optimum thickness was set as 35 nm considering the tradeoff relation between the deposition time and the barrier performance of the inorganic layer.

The thickness of the iCVD pV4D4 layer was also varied to examine the influence of the organic layer thickness on barrier property. It is commonly regarded that the barrier property of the hybrid layer depends mostly on the inorganic layer, while the role of the organic layer only lies in complicating the vapor permeation path, elongating the lag time, and providing mechanical robustness such as flexibility.[22] However, our measurement clearly indicates that a thicker first pV4D4 layer that touches Ca layer directly improved barrier performance substantially, as shown in Figure 3(b). Especially, the improvement of

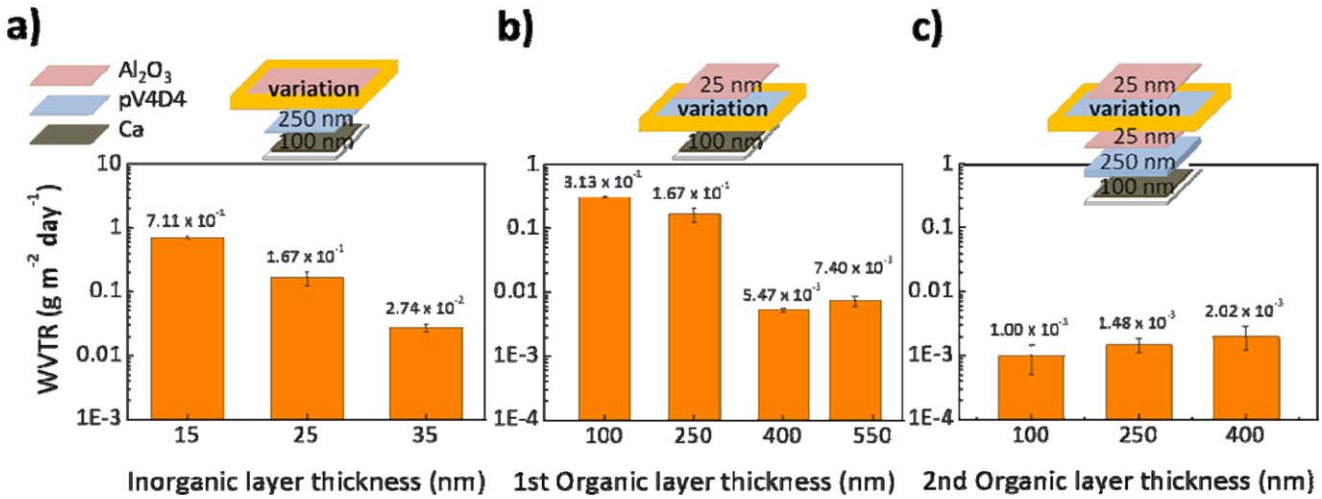

Figure 3. (a) WVTR of 1 dyad of pV4D4/Al_2O_3 hybrid multilayer, with thickness variation of Al_2O_3, fixing the pV4D4 layer thickness at 250 nm. (b) WVTR of 1 dyad of the multilayer, with thickness variation of pV4D4, fixing the Al_2O_3 layer thickness at 25 nm. (c) WVTR of 2 dyads of the multilayer with thickness variation of second pV4D4 layer, fixing the first pV4D4 layer thickness at 250 nm and Al_2O_3 thicknesses at 25 nm. [Color figure can be viewed in the online issue, which is available at wileyonlinelibrary.com.]

the barrier property became significant when the thickness of the very first organic layer was larger than 400 nm. However, the decrease in WVTR value was not evident with further increase of the pV4D4 layer thickness larger than 400 nm, which infers that 400-nm thick organic layer film is a critical threshold thickness to achieve an efficient barrier performance. The thickness of the organic layer in the second hybrid dyad stack was also varied similarly, but no noticeable WVTR deviation was observed [Figure 3(c)]. The result clearly indicates that the first pV4D4 layer contacting the Ca layer directly affects the barrier performance of the organic/inorganic hybrid multilayer immensely, unlike other pV4D4 layers in additional dyads. Although the exact mechanism of this phenomenon is not yet fully understood, it can be assumed that the first pV4D4 layer serves as a protection layer to the underlying Ca layer to minimize the damage to the Ca layer from the following deposition process for the inorganic layer. For example, the diffusion of H_2O molecules to the Ca layer through the first iCVD pV4D4 layer during the ALD process. The thickness of the first pV4D4 layer above 400 nm seems sufficient to prevent the damage from the following deposition process. From above observation, it follows that a thicker first pV4D4 layer is essential for maximizing the barrier property of the hybrid layer, as it serves to block the damage of the Ca layer during the deposition of the following inorganic layer. Our observation on the significance of the first layer thickness is totally consistent with previous reports, where a thicker initial layer is important to achieve superior encapsulation system.[23]

Thus, in this research, the first organic layer was set as above 400 nm. Since the barrier property was indifferent of the thickness of the additional organic layer as shown in Figure 3(c), optimum thickness of the additional organic layer was determined to form reliable interface with inorganic layers and to achieve outstanding flexibility,[24] rather than considering the barrier performance. For reliable and flexible encapsulation, previous reports indicates that the applied organic layer thickness was generally 5–10 times thicker than that of inorganic layer thickness.[24] Since our inorganic layer thickness was chosen as 35 nm, the considered organic layer thickness was in the range 180–350 nm. The deposition rate of the pV4D4 layer was 15 nm/min and we need to minimize the deposition time to maximize the throughput of the barrier fabrication. The stress at the interface during the multilayer fabrication, especially when depositing inorganic layer on organic layer is another critical factor to be thought. When the thickness of organic layer is insufficient, interfacial stress can cause defect, such as crack, on the film. Considering all these factors, we chose 200 nm as the optimized thickness of the 'following' pV4D4 layers to achieve more reliable and highly robust barrier film. Through this structure, an optimum barrier performance could be determined for the organic/inorganic hybrid multilayer.

Optimized Performance of the Organic/Inorganic Hybrid Multilayer

From the systematic control of the layer thickness of each organic and inorganic layer as described above, an optimized barrier structure was determined: the thickness of (1) the first iCVD pV4D4 layer was set as 500 nm, (2) following pV4D4 layers were set as 200 nm, and (3) the ALD Al_2O_3 layer was set as 35 nm. Figure 4(a) displays the SEM image of the organic/inorganic hybrid multilayer with 3 dyads of optimized structure. Each layer was successfully stacked on the substrate without defects or cracks. The interfaces between the organic and inorganic layers formed a tight contact so that no delamination is observed. The interfaces of the layers were stable that no noticeable film damage was observed after 50 times of tape test and exposure to ultrasonication for 90 min. 90°C heat treatment did not cause defects due to thermal expansion as well. The total thickness of the 3 dyads of the hybrid multilayer was around 1 μm. The number of dyads of the optimized organic/inorganic hybrid multilayer was varied from 1 to 3, and the WVTR for each dyad number was calculated, as shown in Figure 4(b). The

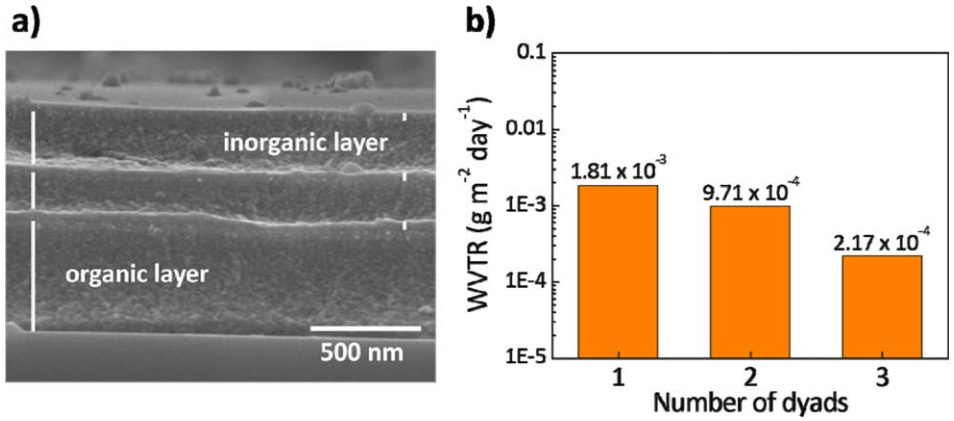

Figure 4. (a) SEM cross-sectional image of the optimized organic/inorganic hybrid multilayer with 3 dyads. (b) WVTR of the optimized multilayers with respect to the increase of the dyad numbers. [Color figure can be viewed in the online issue, which is available at wileyonlinelibrary.com.]

increase in dyad number resulted in a significant improvement of the barrier property. With 3 dyads of the organic/inorganic hybrid layer with the optimized structure, the obtained WVTR value was as low as 2.17×10^{-4} g m^{-2} day^{-1} at 38°C, 90% RH, which corresponds to 1.29×10^{-5} g m^{-2} day^{-1} at ambient condition according to the acceleration relationship suggested by Seo et al.[25] The barrier performance of the 3 dyads of the organic/inorganic hybrid layer was excellent for the encapsulation of organic electronic devices such as OPV and OTFT. The barrier performance can be further improved through optimization of inorganic layer by forming nanolaminate,[19] or through increment of dyad number. The organic/inorganic hybrid multilayer fabricated via iCVD and ALD process can produce a reliable, superior encapsulation system that can elongate the lifetime of organic electronic devices sufficiently for the industrial production.

CONCLUSIONS

In conclusion, we demonstrated a novel method to fabricate organic/inorganic hybrid multilayer using an alternating deposition of organic and inorganic layers by iCVD and ALD systems. The hybrid multilayer showed transparency of higher than 90%, and ignorable loss of light due to cavity effect, since the refractive index, n values of the organic and inorganic layers had marginal difference. A novel Ca test method that measures the oxidized area of Ca layer with respect to time was successfully set up to calculate WVTR values of the multilayers. Then an optimization of the organic/inorganic hybrid multilayer structure was attempted by a systematic change of each organic and inorganic layer to maximize the barrier performance with minimized fabrication time. The Al_2O_3 layer thickness was set as 35 nm while the thickness of the first pV4D4 layer contacting the Ca film directly was set at least larger than 400 nm, and the thickness of the next pV4D4 layers in all dyads were set as 200 nm. Based on the optimized structure, 1–3 dyads of the hybrid multilayers were fabricated and their barrier properties were measured. The optimized hybrid multilayer with 3 dyads was successfully deposited, as confirmed by SEM image. A just 1-μm thick 3 dyads of the organic/inorganic hybrid multilayer showed the WVTR value as low as 2.17×10^{-4} g m^{-2} day^{-1} at 38°C, 90% RH, equivalent to 1.29×10^{-5} g m^{-2} day^{-1} at ambient condition considering the acceleration factors. The combination of iCVD and ALD system proposes a novel, attractive method to produce barrier film with outstanding optical and barrier properties. The iCVD system proves to be the ideal counterpart of the ALD process when depositing organic/inorganic hybrid multilayer since it is a vapor phase deposition, absolutely solvent-free, and plasma-free. Moreover, the similarity in the system of the iCVD and ALD processes can enable us to design a novel system where iCVD and ALD processes are performed in a single-chamber. Thus, further development of the fabrication method can advance the organic electronic industry by presenting multilayer that has barrier and optical properties suitable for encapsulation of the organic electronic devices.

ACKNOWLEDGMENTS

This work was supported by the IT R&D program of MKE/KEIT (Grant No. 10041416, The core technology development of light and space adaptable new mode display for energy saving on 7inch and 2 W), by grant No. EEWS-2014- N01140052 from EEWS Research Project of the KAIST EEWS Research Center. (EEWS: Energy, Environment, Water and Sustainability), and by grant from the Industrial Source Technology Development Program (No. 2010-10038683) of the Ministry of Knowledge Economy (MKE) of Korean government.

REFERENCES

1. Burrows, P. E.; Graff, G. L.; Gross, M. E.; Martin, P. M.; Shi, M. K.; Hall, M.; Mast, E.; Bonham, C.; Bennett, W.; Sullivan, M. B. *Displays* **2001**, *22*, 65.
2. Dennler, G.; Lungenschmied, C.; Neugebauer, H.; Sariciftci, N. S.; Latrèche, M.; Czeremuszkin, G., Wertheimer, M. R. *Thin Solid Films.* **2006**, *511–512*, 349.
3. Burrows, P. E.; Graff, G. L.; Gross, M. E.; Martin, P. M.; Hall, M.; Mast, E.; Bonham, C.; Bennett, W.; Michalski, L.; Weaver, M.; Brown, J. J.; Fogarty, D.; Sapochak, L. S. *Proc. SPIE* **2001**, *4105*, 75.

4. Burrows, P. E.; Bulovic, V.; Forrest, S. R.; Sapochack, L. S.; McCarty, D. M.; Thompson, M. E. *Appl. Phys. Lett.* **1994**, *65*, 2922.
5. Weaver, M. S.; Michalski, L. A.; Rajan, K.; Rothman, M. A.; Silvernail, J. A. *Appl. Phys. Lett.* **2002**, *81*, 2929.
6. Park, J.; Chae, H.; Chung, H. K.; Lee, S. I. *Semicond. Sci. Tech.* **2011**, *26*, 034001.
7. Jung, K. H.; Bae, J.; Park, S. J.; Yoo, S.; Bae, B. *J. Mater. Chem.* **2011**, *21*, 1977.
8. Im, S. G.; Gleason, K. K. *AlChE J.* **2011**, *57*, 276.
9. Tenhaeff, W. E.; Gleason, K. K. *Adv. Funct. Mater.* **2008**, *18*, 979.
10. Lau, K. K. S.; Gleason, K. K. *Macromolecules* **2006**, *39*, 3688.
11. Aresta, G.; Palmans, J.; van de Sanden, M. C. M.; Creatore, M. *Micropor. Mesopor. Mat.* **2012**, *151*, 434.
12. Coclite, A. M.; Ozaydin-Ince, G.; Palumbo, F.; Milella, A.; Gleason, K. K. *Plasma Process Polym.* **2010**, *7*, 561.
13. Perrotta, A.; van Beekum, E. R. J; Aresta, G.; Jagja, A.; Keuning, W.; van de Sanden, R. M. C. M.; Kessels, E. W. M. M.; Creatore, M. *Micropor. Mesopor. Mat.* **2014**, *188*, 163.
14. George, S. M. *Chem. Rev.* **2010**, *110*, 111.
15. Clark, M. D.; Jespersen, M. L.; Patel, R. J.; Leever, B. *J. Org. Electron.* **2014**, *15*, 1.
16. Affinito, J. D.; Eufinger, S.; Cross, M. E.; Graff, G. L.; Martin, P. M. *Thin Solid Films* **1997**, *308–309*, 19.
17. Bertrand, J. A.; George, S. M. *J. Vac. Sci. Technol. A* **2013**, *31*, 01A122.
18. Kim, N.; Potscavage, W. J., Jr.; Sundaramoothi, A.; Henderson, C.; Kippelen, B.; Graham, S. *Sol. Energ. Mat. Sol. C* **2006**, *101*, 140.
19. Seo, S.; Jung, E.; Chae, H.; Cho, S. M. *Org. Electron.* **2012**, *13*, 2436.
20. Seo, S.; Jung, E.; Seo, S. J.; Chae, H.; Chung, H. K.; Cho, S. M. *J. Appl. Phys.* **2013**, *114*, 143505.
21. Lewis, J. S.; Weaver, M. S. *IEEE J. Sel. Topics Quantum Electron.* **2004**, *10*, 45.
22. Chwang, A. B.; Rothman, M. A.; Mao, S. Y.; Hewitt, R. H.; Weaver, M. S. *Appl. Phys. Lett.* **2003**, *83*, 413.
23. Wong, F. L.; Fung. M. K.; Tao, S. L.; Lai, S. L.; Tsang, W. M.; Kong, K. H.; Choy, W. M.; Lee, C. S.; Lee, S. T. *J. Appl. Phys.* **2008**, *104*, 104509.
24. Kim, N.; Graham, S. *Thin Solid Films* **2013**, *547*, 57.
25. Seo, S.; Chae, H.; Seo, S. J.; Chung, H. K.; Cho, S. M. *Appl. Phys. Lett.* **2013**, *102*, 161908.